# Magneto-optical observations of crossing-lattice state in $Bi_2Sr_2CaCu_2O_{8+y}$

M. Yasugaki,[1] K. Itaka,[1] M. Tokunaga,[1,2] N. Kameda,[1] and T. Tamegai[1,2]
[1]*Department of Applied Physics, The University of Tokyo, Hongo, Bunkyo-ku, Tokyo 113-8656, Japan*
[2]*CREST, Japan Science and Technology Corporation (JST), Japan*
(Received 3 April 2002; published 23 May 2002)

The evolution of vortex states and vortex-lattice melting processes in $Bi_2Sr_2CaCu_2O_{8+y}$ under tilted fields are observed a by differential magnetooptical technique. The vortex-lattice melting transitions in the tilted vortex-lattice state and in the crossing-lattice state are found to be similar to each other. When the field is applied at large angles from the *c* axis, the nucleation position of the vortex-liquid paddle is shifted toward the direction of field inclination. The shift of the shielding current leading to the shift of the vortex dome naturally explains the observed phenomena. When a large in-plane field is applied, pancake vortices penetrate through one-dimensional channels starting from a fixed position at the sample edge. We can find a natural explanation for such a feature based on the crossing-lattice ground state.

DOI: 10.1103/PhysRevB.65.212502 PACS number(s): 74.60.Ec, 74.25.Dw, 74.25.Ha, 74.72.Hs

Thermal fluctuations drive the vortex-lattice state to melt into the vortex-liquid state at a first-order phase transition.[1,2] Such phase transitions are experimentally explored in high-temperature superconductors mainly when the external magnetic field is applied parallel to the *c* axis.[3–5] Transitions in the intermediate-field-angle range can be reduced to the transition for the $H//c$ axis in terms of the anisotropic Ginzburg-Landau model when the screening of magnetic field is ignored.[6] In highly anisotropic $Bi_2Sr_2CaCu_2O_{8+y}$ (BSCCO), however, vortex phase transitions occur at low fields ($H < 1000$ Oe) where magnetic screening is effective. As a result, vortex phase transitions in BSCCO show an interesting scaling relation, in which the transition field is suppressed linearly as a function of the in-plane field.[7,8] Koshelev explained this scaling relation based on the crossing-lattice state, in which pancake vortices (PV's) and Josephson vortices (JVs) behave almost independently.[9] Renormalization of the core of JV's by PV's induce effective attractive interactions between these two independent units. The observed mixed chain-lattice state[10,11] is explained by this model, in which extra PV's are attracted to JV's and form chain structure with a higher density of PV's embedded in triangular lattice of PV's.

The melting processes of two distinct vortex solid states, the tilted lattice state and the crossing-lattice state, into the liquid state can be quite different, since the two solid states are separated by a first-order transition.[9] Except for the Bitter decorations,[10,11] no real-space observations of the crossing-lattice state have been available. Recently Soibel *et al.* improved the conventional magneto-optical (MO) technique, to achieve unprecedented field resoluion ($\sim 30$ mG),[12] by subtracting two images taken successively after changing external parameters, such as magnetic field or temperature. We apply the differential MO technique in order to contrast two vortex solid states and explore the nature of crossing-lattice state.

In this Brief Report, we present a comparative study of MO observations on the vortex states in BSCCO under tilted fields in the two different ground states. We also extend these studies to larger in-plane fields, and find one-dimensional structures which only appear in such conditions.

Differential MO images are taken by subtracting images at $H = H_a + \delta H_a/2$ from $H = H_a - \delta H_a/2$, with $\delta H_a \sim 1$ Oe.[12] We use a high-speed-cooled 14-bit CCD camera (Apogee Instruments, 6E) with $1024 \times 1024$ pixels. To achieve-sufficient field resolution ($< 0.1$ G) under a typical background field of 100 G, we need to have a light intensity resolution better than 0.1%. This is achieved by accumulating more than $10^6$ photons into each CCD pixel. We average more than 100 images for each field setting. A bismuth-doped garnet film with in-plane magnetization is used for MO observations.

The crystals used in the present study are grown by the floating-zone method using an image furnace, and are subsequently annealed under a controlled atmosphere to have optimally doped samples with $T_c = 91.7$ K and $\delta T_c < 1.5$ K.[13] These crystals are carefully cleaved to a thickness of about 20 $\mu$m, and cut into approximate dimensions of $500 \times 400 \times 20$ $\mu m^3$ using a wire saw. We always cut the crystal so that the edges are either parallel or perpendicular to the growth direction of the crystal (the *a* axis). In some cases, one of the corners is intentionally cut off to make it easier to identify the orientation of the crystal.

A continuous-flow-type cryostat (Oxford instruments, Microstat) is used for MO observations. In order to apply large magnetic field in two orthogonal directions, we remake the original vacuum shroud and the radiation shield to minimize the size. A small water-cooled electromagnet is used to apply a large in-plane field ($H_x$) up to 6 kOe, while the perpendicular field ($H_z$) is produced by a small air-cooled copper coil up to 500 Oe. When the large in-plane field is applied the Verdet constant of the garnet indicator film is reduced. In some cases, more than 1000 images are averaged to have a reasonable signal-to-noise ratio.

Figures 1(a) and 1(b) compare the vortex-lattice melting processes, with fields nearly parallel to the *c* axis and at an angle of 25° from the *c* axis. The vortex solid-liquid interface shows bow-shaped structures,[14] as already reported.[12,15] They mainly reflect the weak compositional inhomogeneities in the sample, which have been frozen in the crystal during the crystal growth process. According to Koshelev, the vortex system in BSCCO shows a first-order structural phase transition from the tilted lattice state to the crossing-lattice

 

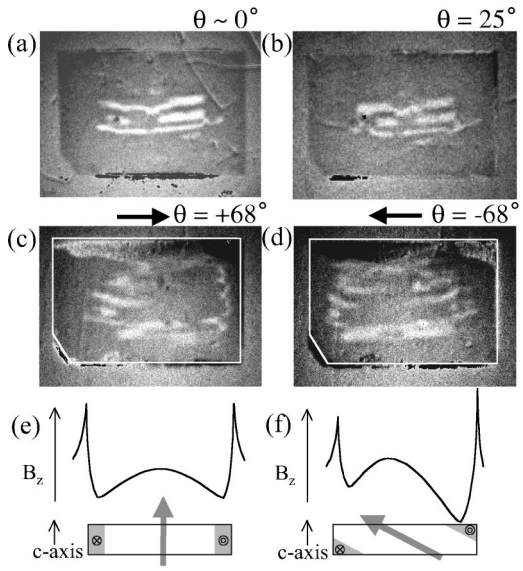


FIG. 1. Comparison of differential MO images of the vortex-lattice melting in BSCCO at $T=70$ K (a) in the tilted-lattice state ($H_z=100$ Oe and $\theta\sim 0°$), and (b) in the crossing-lattice state ($H_z=100$ Oe and $\theta=25°$), where $\theta$ is the field angle from the $c$ axis. White regions forming several one-dimensional rows are the vortex liquid regions. Also shown are differential MO images of the vortex-lattice melting in BSCCO at $T=70$ K near the bulk melting field for two opposite field inclination directions [(c) $\theta=+68°$ and (d) $\theta=-68°$]. Arrows indicate the directions of the in-plane field. The region surrounded by the irregular white boundary is the vortex liquid region. Also shown are schematic cross-sectional views of the shielding-current distribution related to the geometrical barrier (shaded regions) and the resulting $c$-axis field component on the sample surface for (e) $\theta=0°$ ($H//c$ axis) and (f) $\theta=+68°$.

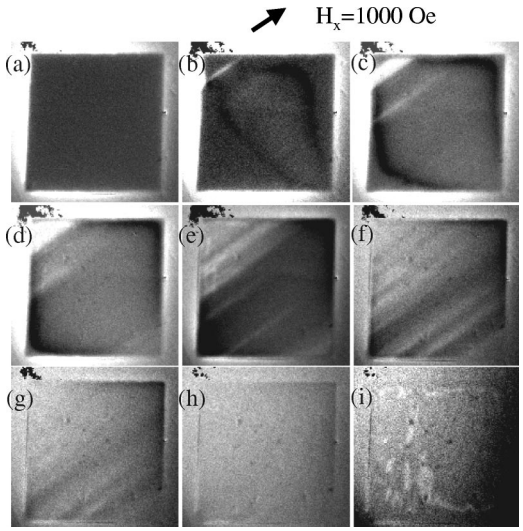


FIG. 2. Evolution of differential MO images at $T=70$ K under a large in-plane field $H_x=1000$ Oe and $H_z=10,15,20,25,30,40,55,65$, and 70 Oe for (a)–(i), respectively. As $H_z$ increases, black boundaries appear perpendicular to $H_x$ (b), expand toward the sample edge [(c) and (d)], and finally disappear (e). At the same time white stripe structures emerge from a fixed position at the edge of the sample (b). A further increase in $H_z$ causes the number of stripes to increase. Before the vortex solid melts into a liquid at $H=70$ Oe (i), the stripes becomes hardly discernible (h).

state at a characteristic angle $\theta_0$ of about 10°, where the angle is measured from the $c$ axis.[9] The transition between these two states is confirmed by the deviation of the linear $H_x$ dependence of the melting field at angles consistent with the theoretical estimate.[16] Although the two images show the melting processes in different ground states, the melting proceeds in a very similar manner. That is, irrespective of the presence of the in-plane field, the melting starts near the center of the crystal. The slight difference in the melting processes in the two ground states is consistent with the smooth crossover from the tilted lattice state to the crossing-lattice state, as are the similar values of the magnetization step at the melting, which is proportional to the entropy change accompanied with the solid to liquid transformation in the two states.[17]

When the field is tilted at large angles, noticeable effects are seen, as shown in Figs. 1(c) and 1(d). The nucleation position of the vortex-liquid puddle slightly shifts from the center of the sample depending on the inclination direction of the field. In a flat superconductor, the shielding current flows all over the sample, in contrast to the slab-shaped superconductor where the shielding current is limited only at the edge. If the pinning is weak in such a superconductor, vortices penetrating into the sample form a dome at the center of the sample, because the shielding current drives the vortices toward the center of the sample. Vortex penetration is delayed by the presence of a geometrical barrier.[18] When the field is applied parallel to the $c$ axis, the edge current flows symmetrically within a range comparable to the thickness of the sample from the edge and produces a symmetric dome profile [Fig. 1(e)]. However, when the field is tilted, the distribution of the edge current will be distorted, as shown in Fig. 1(f). With such an asymmetric edge current distribution, the resulting field profile is readily calculated, as shown in Fig. 1(f). The dome is now shifted slightly toward the direction of the field inclination. This naturally explains the shift of the vortex liquid puddle under a tilted field. It would be instructive to inspect the field distribution in such a condition in more detail. Obviously the vortex dome at the bottom surface is shifted toward the opposite direction compared with the top surface, which is confirmed by a direct observation of the bottom profile (not shown). At this field angle, the vortex system is in the crossing-lattice state, in which PV's and JV's behave independently of each other. However, a flux profile, such as that shown in Fig. 1(f), is incompatible with a simple crossing-lattice picture, where all PV's are expected to be stacked straight, forming vortex lines. In order to produce a flux profile as shown in Fig. 1(f), additional PV's have to be inserted nonuniformly along the $c$ axis. The behavior of such additional PV's will be a subject of future studies.

A further increase in the in-plane field produces several unexpected features. Figure 2 shows the evolution of the differential MO image at $T=70$ K and $H_x=1000$ Oe as a function of $H_z$. At low $H_z$, deep in the vortex solid phase, black boundaries are observed [Figs. 2(b)–2(d)]. With increasing $H_z$ the region surrounded by black boundaries expands, and it finally covers the entire sample [Fig. 2(e)]. At

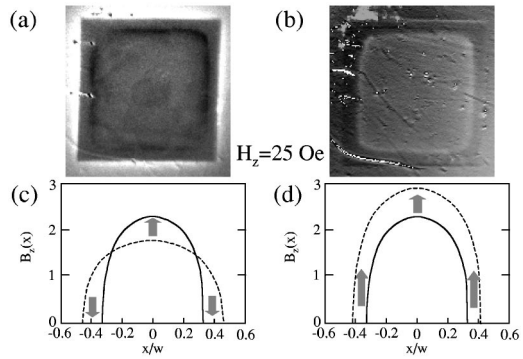


FIG. 3. Comparison of differential MO images in (a) AC and (b) DC modes at $T=70$ K for $H_z=25$ Oe. A schematic change in the local induction is shown when $H_z$ is (c) decreased and (d) increased. Regions with no flux density change (c) are manifested as black boundaries in the AC mode, while the vortex dome is seen as a higher contrast (white) region in (d) as observed in the DC mode.

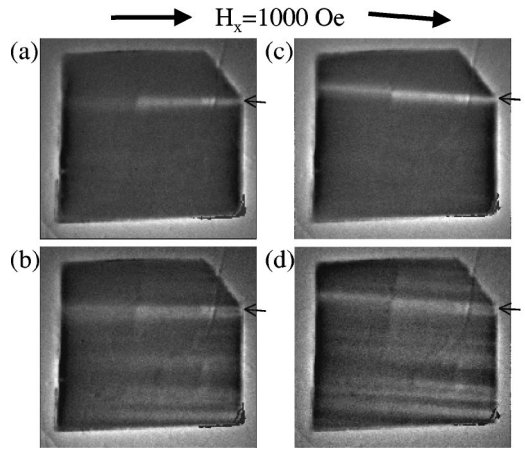


FIG. 4. Comparison of differential MO images at $T=70$ K under $H_x=1000$ Oe for two different directions shown by solid arrows. The out-of-plane field values are $H_z=20$ Oe [(a) and (c)] and 30 Oe [(b), and (d)]. Stripe structures run along the direction of $H_x$ from a fixed position at the sample edge. For example, it nucleates at the same location just below the cut at the upper right corner of the crystal indicated by small arrows for different $H_x$ directions.

the same time, stripelike features start to emerge, and the number of stripes increases with increasing $H_z$. Finally at $H_z=70$ Oe [Fig. 2(i)], the vortex solid melts into a liquid state, again showing a complex nucleation pattern. Let us first discuss the origin of the black boundaries. In our differential MO observations, we make a differential image at two field values, repeat it about 100 times, and finally average the values to construct a better image. We call this way of image acquisition the ''AC mode.'' The same image can, in principle, be obtained by first taking approximately 100 images at $H=H_a$-$\delta H_a/2$ and later taking another 100 images at $H=H_a+\delta H_a/2$ with the risk of instrumental drift over a long time. We call this way of image acquisition the ''DC mode.'' Figure 3 compares the images taken in AC and DC modes. The black boundaries seen in images taken in the AC mode [Fig. 3(a)] turn into white boundaries in images taken in the DC mode [Fig. 3(b)]. The different behaviors in AC and DC modes can be explained by considering the field profile for each field value as shown in Figs. 3(c) and 3(d).[19] In the AC mode, the vortex dome produced at the center of the crystal expands with decreasing field without changing the number of vortices. In this case, the vortex density at the center decreases, while it increases at the edge of the vortex dome [Fig. 3(c)]. On the other hand, in the DC mode, the vortex density in the vortex dome always increases [Fig. 3(d)]. So the differential image shows a higher contrast in the vortex-dome region, which is identified as white boundaries at the edge. Hence it is concluded that the boundaries observed in the differential images are good indicators of the location of the vortex dome.

Next we turn to the stripe features in the images. Figure 4 shows differential MO images taken at $H_x=1000$ Oe and at two $H_z$ values for two different in-plane orientations shown by large arrows in the figure. It is clear that the stripe structures always run along the in-plane field direction.[20] They nucleate at fixed positions on the crystal edge, as indicated by small arrows in the figure. It should be noted that the images shown in Fig. 4 are differential ones. Thus the stripes correspond to regions where the increase in the vortex density upon changing $H_a$ by $\delta H_a$ is grater than the rest of the sample. Since we have a large in-plane field, we start our discussion with a situation where the sample has only a large number of JV's. When we apply $H_z$ in such a sample, PV's will penetrate the sample from the location where the barrier for the penetration is minimum. In weak-pinning flat superconductors, vortices have to overcome the geometrical barrier when they penetrate into the sample through sharp edges.[18] However, the edge of the sample is not perfectly sharp in practice. It has some defects on the order of a few micrometers which facilitate the penetration of vortices. In addition to this, the attractive interactions between PV's and JV's make the barrier at the edges perpendicular to JV's smaller. If the edge of the sample is ideally sharp, PV's penetrate into all JV's uniformly from the sample edges perpendicular to JV's. However, the roughness of the sample edge suppresses the geometrical barrier, and makes the penetration of PV's easier. Even after the field exceeds the average penetration field, more PV's penetrate the sample from such points, and the change in the density of PV's becomes greater compared with the rest of the sample. This causes the image contrast in the stripe structures. It should be noted that in the tilted lattice or vortex chain state as observed in $YBa_2Cu_3O_7$, changes in the external field induce a nearly isotropic increase in the magnetic induction, which is inconsistent with the stripe structures observed in the present experiments. Hence the presence of stripe structures is a fingerprint of the crossing-lattice state realized in highly anisotropic superconductors. The stripe structure becomes weaker and broader as it proceeds from the sample edge, as clearly seen in Fig. 4(b). This fact indicates that PV's gradually spill out of the original stripes as they penetrate deep into the sample.

Finally, let us draw a vortex phase diagram at $T=70$ K for optimally doped BSCCO on the $H_z$-$H_x$ plane based on our MO observations (Fig. 5). The phase diagram of BSCCO under tilted fields is complicated by many anomalies, espe-

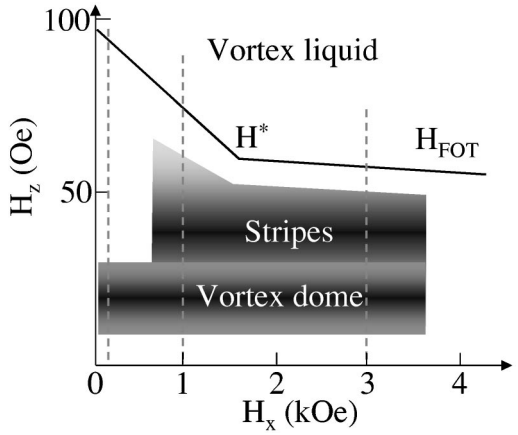


FIG. 5. Schematic phase diagram of BSCCO in the $H_z$-$H_x$ plane based on differential MO observations under tilted fields on the broken lines ($H_x$=100,1000, and 3000 Oe). The solid line is the first-order vortex-lattice melting field ($H_{FOT}$), and $H^*$ is the field where the linear $H_x$ dependence of the melting field breaks down. ''Stripes'' correspond to stripe structures as shown in Figs. 2 and 4. They disappear at $H_z$, slightly lower than the melting field. The ''vortex dome'' is the region where we can identify vortex dome by the black (white) boundaries in the AC (DC) mode.

cially at large $H_x$.[17,21] We overlay each characteristic region of MO observations with a tentative phase diagram determined by the Hall probe.[21] The solid line in Fig. 5 is the first-order vortex-lattice melting field, $H_{FOT}$, and $H^*$ is the field where the linear $H_x$ dependence of the melting field breaks down as determined by Hall probe measurements.[16,22] There are no apparent differences in stripe structures for $H_x$ below and above $H_x^*$. They disappear at $H_z$ slightly lower than the melting field. It is evident that the region with stripe structures roughly covers the region where the vortex system is in the crossing-lattice state ($\theta > 10°$). The stripe structures appear over the entire sample only after the vortex dome covers the entire sample. At small $H_x$(=100 Oe), however, stripe structures are not clearly observed, although the vortex system is still in a crossing-lattice state ($\theta > 45°$). This means that the presence of stripe structures is a sufficient condition for the crossing-lattice state. In this regard, it should be noted that the spacing of the JV's at a typical in-plane field of $H_x$=1000 Oe is about 1 $\mu$m, which is much smaller than the spacing between the stripe structures ($\sim$40 $\mu$m). Also the spacing of the stripes varies with $H_z$ even at a constant $H_x$. These facts indicate that the stripe structures are not directly visualizing vortex chains, as observed by the Bitter decoration experiments.[10,11] Instead, they reflect an inhomogeneous penetration of PV's through rough edges.

In summary, vortex-lattice melting in the tilted-lattice state and in the crossing-lattice state is compared in $Bi_2Sr_2CaCu_2O_{8+y}$ using a differential MO technique. The nucleation of the vortex liquid puddle is found to be insensitive to the change in the ground state of the vortex system. Only at moderate in-plane fields does the shift of the vortex dome make the nucleation of a liquid puddle slightly different depending on the direction of the in-plane field. Under large in-plane fields, stripe structures in the differential images are found to nucleate at specific positions on the sample edge. We interpret this feature as being a direct consequence of the crossing-lattice ground state, where Josephson vortices form one-dimensional channels for pancake vortices.

We thank E. Zeldov for enlightening conversation. This work was supported by a Grant-in-aid for Scientific Research from the Ministry of Education, Culture, Sports, Science, and Technology.

[1] D.R. Nelson, Phys. Rev. Lett. **60**, 1973 (1988).
[2] G. Blatter, M.V. Feigelman, V.B. Geshkenbein, A.I. Larkin, and V.M. Vinokur, Rev. Mod. Phys. **66**, 1125 (1994).
[3] E. Zeldov, D. Majer, M. Konczykowski, V.B. Geshkenbein, V.M. Vinokur, and H. Shtrikman, Nature (London) **375**, 373 (1995).
[4] A. Schilling, R.A. Fisher, N.E. Phillips, U. Welp, D. Dasgupta, W.K. Kwok, and G.W. Crabtree, Nature (London) **382**, 791 (1996).
[5] T. Sasagawa, K. Kishio, Y. Togawa, J. Shimoyama, and K. Kitazawa, Phys. Rev. Lett. **80**, 4297 (1998).
[6] G. Blatter, V.B. Geshkenbein, and A.I. Larkin, Phys. Rev. Lett. **68**, 875 (1992).
[7] S. Ooi, T. Shibauchi, N. Okuda, and T. Tamegai, Phys. Rev. Lett. **82**, 4308 (1999).
[8] J. Mirkovic, S.E. Savel'ev, E. Sugahara, and K. Kadowaki, Phys. Rev. Lett. **86**, 886 (2001).
[9] A.E. Koshelev, Phys. Rev. Lett. **83**, 187 (1999).
[10] C.A. Bolle, P.L. Gammel, D.G. Grier, C.A. Murray, D.J. Bishop, D.B. Mitzi, and A. Kapitulnik, Phys. Rev. Lett. **66**, 112 (1991).
[11] I.V. Grigorieva, J.W. Steeds, and K. Sasaki, Phys. Rev. B **48**, 16865 (1993).
[12] A. Soibel, E. Zeldov, M. Rappaport, Y. Myasoedov, T. Tamegai, S. Ooi, M. Konczykowski, and V.B. Geshkenbein, Nature (London) **406**, 282 (2000).
[13] S. Ooi, T. Shibauchi, and T. Tamegai, Physica C **302**, 339 (1998).
[14] The bow-shaped structures in Fig. 1 happen to run along the in-plane field. However, they have a different origin from the stripe structures shown in Figs. 2 and 4.
[15] T. Tamegai, M. Yasugaki, K. Itaka, and M. Tokunaga, Physica C **357-360**, 568 (2001).
[16] M. Tokunaga, S. Koya, M. Kishi, N. Kameda, K. Itaka, and T. Tamegai, Physica C **357-360**, 446 (2001).
[17] M. Tokunaga, M. Kishi, N. Kameda, K. Itaka, and T. Tamegai (unpublished).
[18] E. Zeldov, A.I. Larkin, V.B. Geshkenbein, M. Konczykowski, D. Majer, B. Khaykovich, V.M. Vinokur, and H. Shtrikman, Phys. Rev. Lett. **73**, 1428 (1994).
[19] N. Morozov, E. Zeldov, D. Majer, and B. Khaykovich, Phys. Rev. Lett. **76**, 138 (1996).
[20] The stripe structures can only been seen in differential images, since the local induction modulation is a small ripple superimposed on the large dome profile.
[21] T. Tamegai, M. Tokunaga, M. Kishi, S. Koya, N. Kameda, and K. Itaka, Physica C **364-365**, 499 (2001).
[22] S. Ooi, T. Shibauchi, K. Itaka, N. Okuda, and T. Tamegai, Phys. Rev. B **63**, 020501 (2001).